Subcellular recruitment by TSG118 and TSPYL implicates a role for zinc finger protein 106 in a novel developmental pathway

ARTICLE *in* THE INTERNATIONAL JOURNAL OF BIOCHEMISTRY & CELL BIOLOGY · AUGUST 2005

Impact Factor: 4.05 · DOI: 10.1016/j.biocel.2005.01.013 · Source: PubMed

Available online at www.sciencedirect.com
SCIENCE DIRECT®
ELSEVIER
The International Journal of Biochemistry & Cell Biology 37 (2005) 1421–1437
IJBCB
www.elsevier.com/locate/biocel

Subcellular recruitment by TSG118 and TSPYL implicates a role for zinc finger protein 106 in a novel developmental pathway

Helmut Grasberger*, Graeme I. Bell

Departments of Biochemistry and Molecular Biology, and of Medicine and Human Genetics, The University of Chicago, Chicago, IL 60637, USA

Received 4 November 2004; received in revised form 25 January 2005; accepted 26 January 2005

Abstract

To gain insight into the function of zinc finger protein 106 (ZFP106), we analyzed its subcellular targeting and identified its interacting proteins. Although ZFP106 was detected predominantly in the fibrillar component of the nucleolus and co-localized with the nucleolar transcriptional machinery, its overexpression did not affect transcription of pre-ribosomal RNA genes. The nucleolar association of ZFP106 did neither require ongoing ribosomal RNA synthesis nor nucleolar chromatin indicating that a protein–protein interaction confines ZFP106 to the nucleolus. Deletion analysis revealed that the C-terminal WD40 repeat region functions in nucleolar targeting. This domain interacts with the product of testis-specific gene 118 (TSG118), which also co-localizes with ZFP106 in the nucleolus. Rapid downregulation of TSG118 expression during in vitro terminal differentiation coincides with a loss of nucleolar ZFP106. By its structural features and expression, TSG118 mimics nucleostemin, a nucleolar protein linked to the proliferation potential of stem cells. A two-hybrid screen with the N-terminal region of ZFP106 as bait led to the isolation of testis-specific Y-encoded-like protein (TSPYL), a member of the nucleosome assembly protein family. A frame-shift mutation in TSPYL has recently been found to cause a sudden infant death syndrome with testis dysgenesis. Specific recruitment of ZFP106 via amino acids 412–781 into TSPYL-positive nucleoplasmic bodies requires a TSPYL domain absent in the mutant protein of patients with testis dysgenesis. These results identify ZFP106 as a potential player in a novel pathway involved in testis development.

Keywords: Nucleolus; Differentiation; Testis development; Nucleosome assembly protein; Nucleolar sequestration

Abbreviations: CLSM, confocal laser scanning microscopy; DFC, dense fibrillar component; FC, fibrillar centers; GC, granular component; GFP, green fluorescent protein; NAP, nucleosome assembly protein; NLS, nuclear localization signal; PBS, phosphate-buffered saline; XP, XPress epitope

* Corresponding author. Present address: Department of Medicine, The University of Chicago, 5841 South Maryland Avenue, MC3090, Chicago, IL 60637, USA. Tel.: +1 773 702 9273/6939; fax: +1 773 702 6940.
E-mail address: hgrasber@uchicago.edu (H. Grasberger).

1357-2725/$ – see front matter © 2005 Elsevier Ltd. All rights reserved.
doi:10.1016/j.biocel.2005.01.013

1. Introduction

The nucleolus is the most prominent subnuclear domain of eukaryotic cells and the site of transcription of the clustered pre-ribosomal RNA genes (rDNA), subsequent processing of precursor rRNA and their assembly into pre-ribosomal particles. Ultrastructurally, the nucleolus is composed of three distinct compartments: regions with fibrillar appearance, called fibrillar centers (FC), which contain the tandemly repeated rRNA genes as well as proteins essential for rRNA transcription such as RNA polymerase 1 and upstream binding factor 1; more densely stained regions rich in fibrillarin and other rRNA processing factors surrounding the FC and termed the dense fibrillar component (DFC); and the particle-rich granular component (GC). Pre-ribosome biogenesis follows a vectorial process initiating with the transcription of rRNA genes at the border of FC and DFC and progressing outward through the DFC to the GC as the primary rRNA is processed, modified, and assembled into pre-ribosomal particles (Scheer & Hock, 1999).

In recent years, numerous studies demonstrated that the nucleolus is involved in other regulatory functions not related to ribosome biogenesis. Proteomics studies revealed that the majority of identified nucleolar proteins are not related to ribosome biosynthesis and that certain proteins associate with the nucleolus only under specific conditions (Andersen et al., 2002; Scherl et al., 2002). Nucleolar sequestration of proteins has now been recognized as a common control mechanism, allowing temporary storage and subcellular confinement of proteins (Visintin & Amon, 2000). For example, regulation by nucleolar sequestration has been described for the p53 ubiquitin ligase Mdm2 (Bernardi, Scaglioni, Bergmann, Horn, Vousden, & Pandolfi, 2004; Weber, Taylor, Roussel, Sherr, & Bar-Sagi, 1999; Zhang & Xiong, 1999), the cell-cycle regulator Cdc14 (Shou et al., 1999), and transcription factors such as hypoxia-inducible factor (Fatyol & Szalay, 2001; Mekhail, Gunaratnam, Bonicalzi, & Lee, 2004) and the transcriptional repressor Daxx (Lin & Shih, 2002).

Following import across the nuclear pore complex, confinement of a protein in a non-membrane-bound steady-state compartment, such as the nucleolus, is generally mediated by interaction with local high-affinity binding sites (Misteli, 2001). Thus, it is currently accepted that domains necessary for nucleolar targeting of a molecule function by their direct or indirect interaction with the rDNA or rRNA constituents of the nucleolus (Jacobson, Cao, Wang, & Pederson, 1995; Shaw & Jordan, 1995; van Eenennaam, van der Heijden, Janssen, van Venrooij, & Pruijn, 2001).

Zinc finger protein 106 (ZFP106) was initially cloned as the polymorphic gene encoding the nine amino acid H3a minor histocompatibility transplantation antigen (Zuberi, Christianson, Mendoza, Shastri, & Roopenian, 1998). We have characterized the complete structures and transcriptional regulation of the human and mouse ZFP106 genes (Grasberger, Hong gang, Mashima, & Bell, 2005). ZFP106 expression is directed from two separate promoter regions (P1 and P2), driving expression of proteins with distinct N-termini. P1 is active during embryogenesis as well as in proliferating somatic cell lines. In contrast, activation of the P2 promoter is strictly coupled to myogenic differentiation. The P1-derived ZFP106 protein is predicted to contain N- and C-terminal tandem zinc finger structures, the latter preceded by a seven WD40 repeats domain. Outside these frequently observed domains, ZFP106 bears no significant amino acid homology to other proteins of known function. Thus, sequence analysis of ZFP106 has failed to provide a direct clue to its function.

One approach to gain insight into the physiological functions of ZFP106 lies in the characterization of its subcellular localization and the identification of interacting proteins. The results presented here identify ZFP106 as a previously unrecognized constituent of the nucleolus in somatic cell lines. The C-terminal domain comprising the WD40 repeats confines ZFP106 to the fibrillar regions of the interphase nucleolus by interaction with testis-specific protein 118 (TSG118) (Larsson, Brundell, Jorgensen, Stahl, & Hoog, 1999). The structural features and expression profile of TSG118 closely resemble those of nucleostemin, a nucleolar protein involved in the control of the proliferation potential of stem cells (Tsai & McKay, 2002). Akin to the regulation of nucleostemin in neuronal stem cells, TSG118 expression is rapidly downregulated upon induction of terminal differentiation in myoblasts coinciding with loss of nucleolar targeting of ZFP106. We also provide evidence that ZFP106 is recruited to nuclear bodies by testis-specific Y-encoded-like protein (TSPYL), an ubiquitously expressed, putative transcriptional regulator, whose loss in humans has

recently been found to cause sudden infant death syndrome with testis dysgenesis (SIDDT) (Puffenberger et al., 2004).

2. Materials and methods

2.1. Cell culture

COS-7, HEK293, HeLa, HepG2, and NIH 3T3 cells were maintained in Dulbecco's modified Eagle's medium (DMEM) supplemented with 2 mM L-glutamine, 4.5 g/l D-glucose, and 10% fetal bovine serum (FBS). Mouse C2C12 myoblasts were grown at low density in the same medium except for supplementation with 20% FBS to prevent differentiation. To induce terminal differentiation, C2C12 cells grown to ~80% confluence were switched to medium supplemented with 2% horse serum instead of 20% FBS.

2.2. Antibodies

An N-terminal GST-fusion protein of amino acids 1815–1888 of murine ZFP106 (accession no. AAD04329) was expressed in *Escherichia coli* BL-21, purified by glutathione-sepharose (Amersham Biosciences) chromatography and used to raise antisera in rabbits. The antibodies (anti-ZFP106/C) were affinity purified as described (Hall et al., 1984). Epitope-tagged constructs were detected with mouse anti-XPress (anti-XP) (Invitrogen), rat anti-HA clone 3F10 (Roche), rabbit anti-c-myc (Covance) or monoclonal mouse anti-c-myc (CLONTECH). The primary antibodies for labeling subnuclear structures were human autoimmune sera against fibrillarin, B23, and RNA polymerase 1 (all from SLR Research), and mouse anti-PML clone M3 (Santa Cruz).

2.3. Expression constructs

The coding regions for the four major Zfp106 splice isoforms (Fig. 1) (Grasberger et al., 2005) were amplified by RT-PCR from murine heart RNA and each inserted into the expression vector pcDNA4/His (Invitrogen) to direct expression of N-terminal XP-tagged fusions of the ZFP106 proteins. Deletion constructs were created by subcloning of fragments of the aforementioned constructs with the help of natural or PCR-generated restriction sites. The sequences of

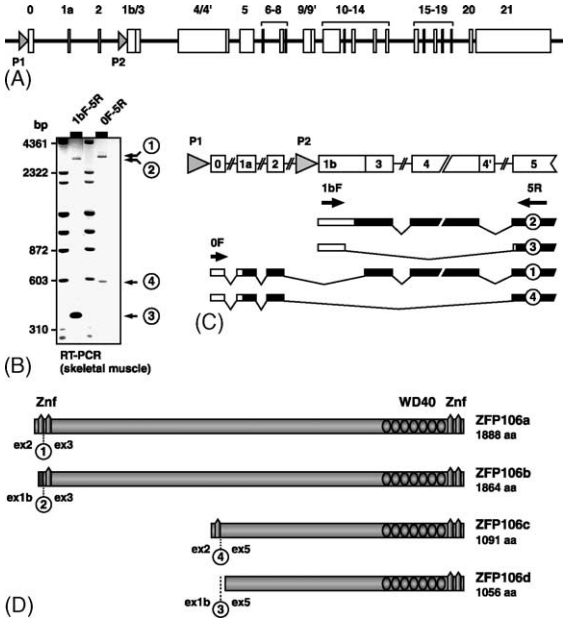

Fig. 1. Alternative splicing of ZFP106 generates four major isoforms. (A) Gene structure of ZFP106 and location of the P1 and P2 promoter regions. (B) RT-PCR demonstrating alternative splicing of the exons 3 and 4 region for both P1- and P2-derived transcripts. (C, D) Schematic of the four major ZFP106 transcripts and the predicted ZFP106 protein isoforms.

all constructs were confirmed. The cDNAs of the four ZFP106 isoforms, including the XP epitope encoding 5′-end, were also utilized to construct replication-deficient, recombinant adenovirus using the Adeno-X Tet-off system according to the manufacturer's protocol (CLONTECH). A control virus contained the coding sequence for XP-tagged β-galactosidase, subcloned from pcDNA4-LacZ (Invitrogen). Adenovirus was purified by double cesium gradient banding. Target cells were simultaneously infected with a regulatory virus (Adeno-X Tet-off, CLONTECH) and one of the recombinant ZFP106 adenovirus, each at a multiplicity of infection of ten. Expression of the recombinant proteins was suppressed by adding 1 μg/ml doxycycline to the culture medium and maximally induced by changing to doxycycline-free medium.

2.4. Subcellular fractionation, nuclear matrix isolation, and in situ fractionation

To prepare nuclei, washed HeLa cells were swollen for 10 min on ice in hypotonic buffer (10 mM Tris–HCl,

pH 7.4, 10 mM NaCl, 10 mM $MgCl_2$, 0.5% NP-40, 0.5 mM phenylmethylsulfonyl fluoride), vortexed, and nuclei pelleted at 750 g for 10 min. The supernatant was further clarified by centrifugation at 20 000 × *g* and designated the (soluble) cytoplasm-containing fraction (cyt). The nuclei-containing pellet was washed twice in hypotonic buffer and designated the nuclei-containing fraction (nuc). For subnuclear fractionation, the nuclei were resuspended in digestion buffer (50 mM Tris, pH 7.4, 250 mM sucrose, 5 mM $MgSO_4$) and the chromatin digested for 1 h at 4 °C with 40 units RNase-free DNase-1 (Roche) per ~10^6 cells. The supernatant obtained after centrifugation at 800 × *g* was designated S1-DNase. To remove the digested chromatin, the nuclei were resuspended in 10 mM Tris–HCl, 0.2 mM $MgSO_4$ and extracted by stepwise addition of sodium chloride to a final concentration of 1.6 M and further incubation for 15 min on ice. The supernatant after centrifugation at 3000 × *g* was designated S2 (high salt extraction) and the pellet the nuclear matrix fraction (NM). Aliquots of the different fractions corresponding to an equivalent portion of the original cell homogenate were analyzed by Western blotting using standard procedures (Sambrook, Fritsch, & Maniatis, 1989). For in situ fractionation, cell monolayers were sequentially extracted according to the method of He, Nickerson, and Penman (1990).

2.5. Indirect immunofluorescence

Cells were fixed for 20 min at room temperature in 4% paraformaldehyde/phosphate-buffered saline (PBS), and then permeabilized for 5 min with 0.2% Triton X-100/PBS. Nonspecific binding sites were blocked with 3% bovine serum albumin/1% goat serum/PBS. After incubation with primary antibody(s) (listed under Section 2.2), appropriate affinity-purified anti-IgG labeled with either Alexa Fluor 488 or Alexa Fluor 568 were used as secondary reagents (all from Molecular Probes). After staining of DNA with Hoechst 33342 fluorochrome, the slides were mounted with Prolong antifade (Molecular Probes). Conventional and confocal images were taken with a Nikon Eclipse E800 microscope equipped with PCM-2000 (Nikon, New York, NY). Each construct was analyzed in a minimum of three independent transfections.

2.6. Nucleolar run-on transcription assay

Run-on transcription in permeabilized HeLa cells was performed according to the method described by Wansink, Schul, van der Kraan, van Steensel, van Driel, and de Jong (1993) with modifications to increase specificity for RNA polymerase 1 (Gebrane-Younes, Fomproix, & Hernandez-Verdun, 1997). Briefly, cells were washed in PBS and permeabilization buffer (20 mM Tris–HCl, pH 7.4, 5 mM $MgCl_2$, 0.5 mM EGTA, 0.5 mM PMSF), followed by incubation for 5 min at room temperature in the same buffer containing 0.05% Triton X-100. After extensive washes in permeabilization buffer without Triton X-100, cells were incubated in run-on buffer (50 mM Tris–HCl, pH 7.4, 100 mM KCl, 5 mM $MgCl_2$, 0.5 mM EGTA, 25 μM *S*-adenosyl-L-methionine, 0.5 mM of each ATP, CTP, and GTP, and 0.2 mM Br-UTP) supplemented with 50 μg/ml α-amanitin. Following two washes in PBS containing 5 units/ml RNase inhibitor (Ambion), the cells were fixed and permeabilized as described above. A monoclonal antibody to Br-deoxyuridine (Sigma) was used as primary antibody to detect transcription.

2.7. Yeast two-hybrid library screening and interaction assay

Yeast two-hybrid library screening and interaction assays were conducted with the Gal4-based MATCHMAKER System 3 (CLONTECH) according to the manufacturer's recommendations. Briefly, a PCR-amplified cDNA fragment encoding residues 1527–1888 of murine ZFP106 was cloned via *Eco*RI and *Sal*I in frame to the Gal4 DNA-binding domain of pGBKT7 to generate BD-ZFP106 (1527–1888). This bait vector was transformed into yeast strain AH109 (MATa), which was then mated with strain Y187 (MATα), which had been pre-transformed with a mouse embryonic day 11 cDNA library generated in plasmid pACT2. Of ~1.3×10^7 independent double transformants screened, 56 colonies were selected after three rounds of selection based on their confirmed ability to survive quadruple selection (His, Ade, Leu, Trp) and express β-galactosidase. For the second library screen, a PCR-amplified cDNA fragment encoding residues 240–834 of human ZFP106 was cloned as translational fusion of the Gal4 DNA-binding domain into the *Bam*HI site of pGBKT7. This bait construct

was used in a screen of $\sim 0.5 \times 10^6$ clones of a human skeletal muscle library, resulting in the isolation of four β-galactosidase-positive clones surviving quadruple metabolic selection. For both interaction screens, the pACT2 plasmids of all positive clones were rescued in *E. coli* and their inserts analyzed by sequencing.

2.8. Co-immunoprecipitation

HeLa cell nuclei were isolated essentially as described (Schreiber, Matthias, Muller, & Schaffner, 1989) and extracted at 4 °C with 400 mM NaCl in 20 mM Hepes, pH 7.5, 1 mM EDTA, 1 mM EGTA, 1 mM DTT and proteinase inhibitors (Complete, ROCHE). Extracts were diluted, pre-cleared with protein-A sepharose (Amersham Biosciences) and subjected to immunoprecipitation according to standard protocols (Harlow & Lane, 1988).

3. Results

3.1. Identification of ZFP106 as a novel nucleolar protein

Expression of ZFP106 is directed from two distinct promoter regions, P1 and P2, which drive ubiquitous and striated muscle-specific expression, respectively (Grasberger et al., 2005) (Fig. 1A). In both cases, exons 3 and 4 can be removed from the primary transcripts by analogous alternative splicing events leading to four major isoforms (Fig. 1B–D). To study the subcellular localization of ZFP106, we prepared expression constructs encoding an N-terminal XP-epitope fused to the coding regions of the four ZFP106 cDNAs isolated from a murine heart cDNA library. Expression of these constructs was first assessed by coupled in vitro transcription/translation. As shown in Fig. 2A, the ZFP106a construct directed expression of a protein with apparent molecular weight of ~260 kDa, i.e. substantially higher than the 210 kDa predicted from the amino acid sequence (including the epitope tag).

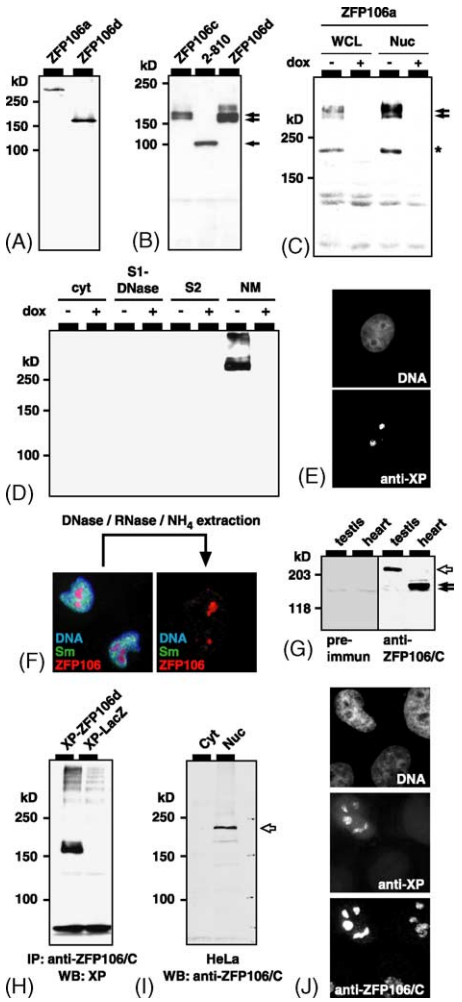

Fig. 2. Identification of ZFP106 as a nucleolar protein. (A) ^{35}S-labeled ZFP106a and ZFP106d were expressed in reticulocyte lysate system and analyzed on SDS-PAGE. (B) Expression of ZFP106 isoforms in transient transfected HeLa cells. Recombinant proteins were detected by their N-terminal XP epitope tag. (C) Expression of ZFPP106a using recombinant adenovirus Tet-Off expression system. Tetracycline in the culture medium suppresses expression of recombinant ZFP106a. The asterisk indicates a frequently observed degradation product. (D) Biochemical fractionation of XP-ZFP106a. Cyt, cytoplasm; S1-DNase, extraction following digestion of DNA; S2, high salt extraction; NM, nuclear matrix fraction. (E) Indirect immunofluorescence of ZFP106a in transfected HeLa cells. (F) ZFP106a remains in the nucleolus after in situ nuclear fractionation, whereas Sm (an snRNP component of splicing speckles) and genomic DNA are completely extracted. (H) Whole cell extracts of HeLa cells transfected with either XP-ZFP106d or XP-LacZ expression vectors were subjected to immunoprecipitation with antibodies to the ZFP106 C-terminus (anti-ZFP106/C), and the precipitated protein analyzed by immunoblot with XP antibody. (I) Detection of a ~210 kDa endogenous ZFP106 protein by anti-ZFP106/C in the nuclear fraction of HeLa cells. (J) Indirect immunofluorescence of non-transfected HeLa cells using anti-ZFP106/C. (G) Western blot of adult mouse tissues using anti-ZFP106/C reveals a ~210 kDa protein in testis, but a ~170 kDa protein in heart (and all other tissues tested; not shown).

Likewise, ZFP106d (Fig. 2A) and the other two ZFP106 isoforms (not shown) migrated substantially slower on SDS-PAGE than expected from their calculated molecular weight, and, in all cases, phosphatase treatment of the in vitro translated proteins did not correct the anomalous migration (not shown).

When the same constructs were transiently transfected in somatic cell lines (HeLa, COS7, HEK293), the apparent molecular weight of ZFP106c and ZFP106d agreed well with that of the in vitro translated products. Both ZFP106c and ZFP106d were detected as distinct double bands (Fig. 2B), a phenomenon preserved after phosphatase treatment (not shown) and not observed by expression of ZFP106 fragments lacking the C-terminal WD40/zinc finger domain (compare Fig. 5C). In contrast, full-length ZFP106 isoforms (i.e. ZFP106a and ZFP106b) were barely detectable by Western blotting following transient transfections (not shown). Using an inducible (Tet-Off) recombinant adenovirus system, expression of both ZFP106a and ZFP106b was detectable in the various cell lines tested (HeLa, HepG2, HEK293, C2C12, COS7), but was still remarkably low compared to the viral expression of the two smaller ZFP106 isoforms. We detected again a double band (of ~260/270 kDa) and the size of the smaller band was consistent with that of the in vitro translated product (Fig. 2C). The mechanism preventing expression of ZFP106a or ZFP106b at higher levels in tissue culture cells remains to be clarified. There was no obvious increase in cellular toxicity of the viral constructs, which could account for the low expression level.

Further investigation of ZFP106 expression by subcellular fractionation revealed that ZFP106a expressed in HeLa cells was exclusively found in the nuclear fraction and not extracted by detergents, digestion of chromatin, and subsequent high salt extraction (Fig. 2D), indicating that ZFP106 fractionated with the operationally defined nuclear matrix. Such insolubility was also found for the other three ZFP106 isoforms, but not an N-terminal truncated ZFP106 (amino acids 2–810 of ZFP106b), which was recovered in the soluble nuclear fraction (not shown). This implies that the region encompassing amino acids 833–1888, that is common to all four isoforms, determines association with the nuclear matrix. The results of the biochemical fractionation were confirmed by indirect immunofluorescence showing nuclear localization of all four ZFP106 isoforms. More specifically, the immunofluorescence signals appeared as unsymmetrically dots-like structures within round-shaped regions lacking staining with the DNA-intercalating Hoechst 33342 dye, suggesting that ZFP106 was targeted to the nucleoli (Fig. 2E). In situ fractionation confirmed the association of ZFP106 with the nucleolar matrix (Fig. 2F). Digestion of RNA prior to high salt extraction also indicated that the nucleolar localization of ZFP106 did not require the RNA component of the nuclear matrix.

To investigate the expression of endogenous ZFP106 proteins, we generated polyclonal antibodies (anti-ZFP106/C) to the C-terminal residues 1815–1888 of ZFP106. When tested by Western blotting of in vitro translated proteins, anti-ZFP106/C reacted with all ZFP106 isoforms, but not a C-terminal truncated ZFP106 fragment lacking the epitope region (not shown). XP-ZFP106d, but not XP-LacZ, was detected by XP antibody in the anti-ZFP106/C immunoprecipitates of cells transfected with the corresponding constructs (Fig. 2H). Anti-ZFP106/C reacts with an endogenous ~210 kDa protein of the nuclear fraction of HeLa cells (Fig. 2I), which by subnuclear fractionation was shown to be a constituent of the nuclear matrix (not shown). When tested on a panel of mouse tissue extracts, the size of the protein detected by anti-ZFP106/C varied between 170–180 kDa in the tissues examined (data shown for heart in Fig. 2G). This differs in testis where the protein detected is identical in size (210 kDa) to that found in HeLa cells or other transformed cell lines. Indirect immunofluorescence of HeLa and COS-7 cells with anti-ZFP106/C revealed a specific nucleolar signal (Fig. 2J) not observed by staining with pre-immune serum. Pre-adsorption of anti-ZFP106/C by excess of the GST-ZFP106 (1815–1888) immunogen, but not GST alone, eliminated the nucleolar staining (not shown). Anti-ZFP106/C immunolabeling showed enhanced nucleolar signal in all cells transfected with XP-ZFP106a and, in double immunolabeling with XP and anti-ZFP106/C, the staining patterns with both antibodies were coincident (Fig. 2J). Taken together, both endogenous and exogenous ZFP106 are detected in the nucleolar matrix of somatic cell lines. Our transfection experiments suggest that the full-length ZFP106 isoforms (ZFP106a and ZFP106b) are unstable and probably subject to proteolytical processing by unknown protease(s), which would be consistent

with our failure to detect an endogenous protein of the expected full-length size in various cell lines or tissues known to express substantial amounts of the corresponding mRNA (Grasberger et al., in press).

3.2. ZFP106 localizes to the fibrillar components of the nucleolus

As mentioned earlier, the nucleolus is composed of three electron microscopically defined substructures, which correspond to distinct processing steps of the ribosome synthesis pathway. We therefore delineated the position of ZFP106 relative to marker proteins of nucleolar substructures using double immunolabeling confocal laser scanning microscopy (CLSM). In interphase nucleoli, ZFP106 substantially co-localizes with RNA polymerase 1 and fibrillarin, marker proteins for the FC and surrounding DFC, respectively, but not nucleophosmin/B23, a constituent of the GC (Fig. 3A). Thus, ZFP106 is part of the fibrillar components of the nucleolus and, if involved in ribosome synthesis, may play a role in either rDNA transcription or early processing steps of the 45S precursor rRNA, but not in the subsequent assembling of the ribosomal particles.

3.3. Nucleolar localization of ZFP106 does not require ongoing rRNA transcription

To further investigate the structural requirements for the nucleolar localization of ZFP106, we studied the subcellular localization of ZFP106 after selective inhibition of RNA polymerase 1 by low doses (0.05 μg/ml) of the DNA-intercalating agent actinomycin D, a treatment that segregates the normally interspersed fibrillar and granular components of the nucleolus (Yokoyama, Niwa, & Tamaya, 1992). Both XP-ZFP106a (Fig. 4A) and XP-ZFP106d (not shown) exhibited a clear redistribution from non-symmetrical nucleolar dots before drug-treatment to the nucleolar periphery after drug-treatment, forming peri-nucleolar caps. RNA polymerase 1 and fibrillarin both co-localized with ZFP106a in the segregated nucleoli (Fig. 4A). These cap-like structures have been previously shown to contain the nucleolus organizer regions, i.e. the clustered rRNA genes, which are retracted to the nucleolar perimeter upon actinomycin D treatment. Hence, targeting of ZFP106a to the fibrillar components does not require ongoing rRNA synthesis.

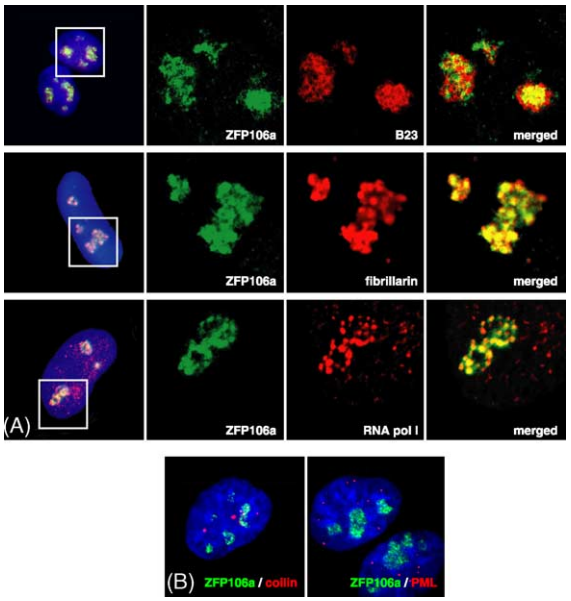

Fig. 3. ZFP106 is recruited to the fibrillar components of the nucleolus. (A) HeLa cells were infected with recombinant adenovirus expressing XP epitope tagged ZFP106a. Cells were fixed 24 h after infection and the subcellular localization of ZFP106a (second column, in green) was analyzed in relation to the nucleolar marker proteins (third column, in red) B23/nucleophosmin, fibrillarin, and RNA polymerase 1 by CLSM. Regions of co-localization appear in yellow in the overlays (merged; fourth column). Corresponding conventional epifluorescence images are depicted in the first column, with the DNA stained using Hoechst 33342 dye (in blue). (B) ZFP106 does not localize to Cajal bodies (coilin) or PML nuclear bodies (PML).

To identify the distribution of ZFP106 relative to actual rDNA transcription sites, an RNA polymerase 1-specific in situ run-on assay was performed based on BrUTP incorporation into nascent rRNA transcripts and subsequent detection by immunofluorescence with anti-BrdU. ZFP106 localized predominantly adjacent to the accumulating rRNA transcripts, which can be observed as frequently necklace-like configured dots in the interior of the nucleoli (Fig. 4B). Overexpression of ZFP106a or ZFP106d did not affect distribution or signal strength of the newly synthesized rRNA.

3.4. Mapping of nuclear and nucleolar-targeting domains of ZFP106

To delineate the structural elements involved in subcellular targeting of ZFP106, deletion constructs were

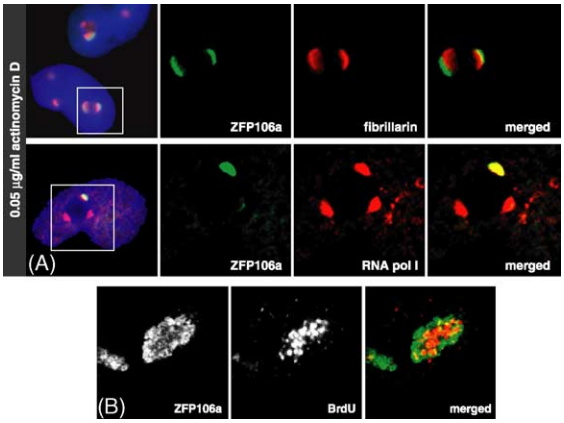

Fig. 4. Ribosomal RNA synthesis is neither required for recruitment of ZFP106 nor affected by ZFP106 overexpression. (A) HeLa cells transfected with a vector encoding XP-tagged ZFP106a were treated with 0.05 μg/ml actinomycin D for 1 h to inhibit RNA polymerase 1 transcription. Fixed cells were double-immunostained with XP (green) and either anti-fibrillarin or anti-RNA polymerase 1 (both shown in red). First column: conventional fluorescence images, DNA stained with Hoechst 33342 (blue). Overlays (merged) of enlarged confocal images of ZFP106 with those of fibrillarin or RNA polymerase 1 reveal association of ZFP106 with the rDNA transcriptional complex independent of ongoing rRNA synthesis. (B) By in situ nuclear run-on assay, overexpression of ZFP106a (or ZFP106d) does not abolish transcription of rDNA. ZFP106a localizes predominantly adjacent to the accumulating rRNA transcripts, which are detected by indirect immunofluorescence of incorporated BrUTP with anti-BrdU (BrdU).

expressed in COS7 cells (Fig. 5A and C) and analyzed by indirect immunofluorescence (Fig. 5D). ZFP106a and ZFP106b localized exclusively to the nucleolus in more than 95% of transfected cells. Residues 803–819 (RRNVNWEQVIQQVTKKK) conform to the consensus for a bipartite nuclear localization signals (NLS). However, N-terminal ZFP106 deletions (comprising

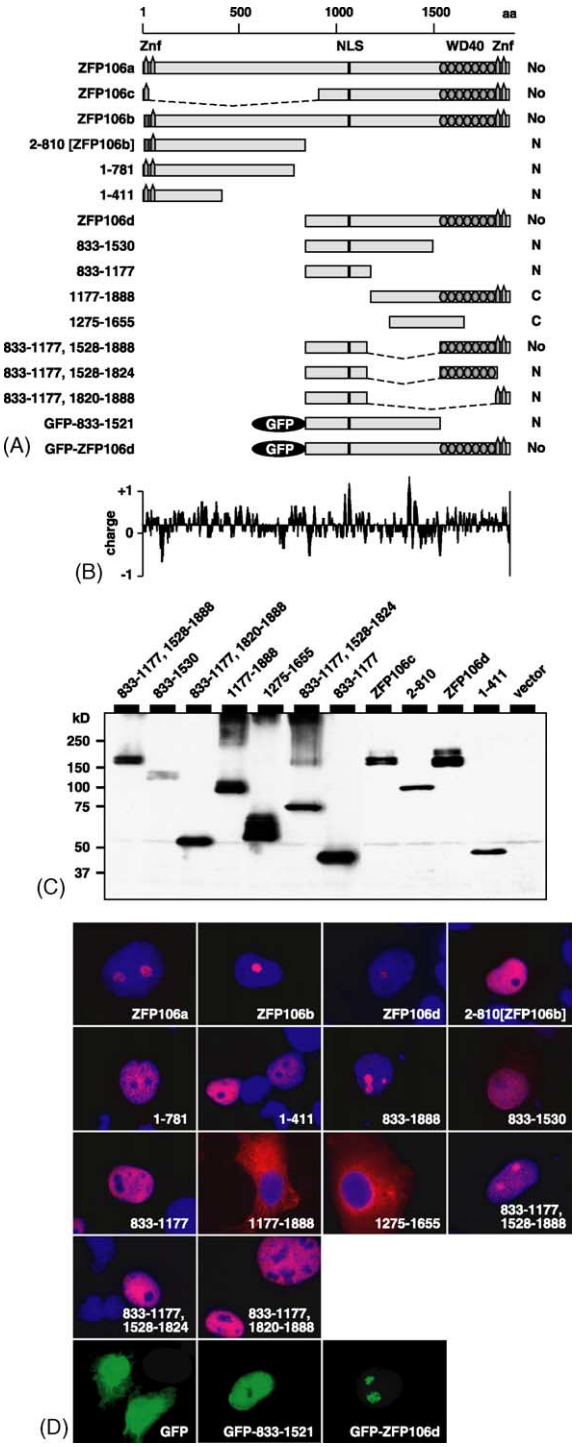

Fig. 5. Deletion mapping of nuclear and nucleolar-targeting domains. (A) The series of deletion constructs analyzed for subcellular localization. C, cytoplasmic; N, nucleoplasmic with nucleolar exclusion; No, (predominantly) nucleolar. (B) Charge density plot aligned to the constructs in (A). (C) Western blot analysis of the deletion constructs expressed in COS-7 cells using anti-XP antibody. (D) ZFP106 deletion constructs were expressed in COS-7 cells and their subcellular localization visualized by indirect immunofluorescence (red color). DNA counterstained with Hoechst 33342 (blue). Amino acids 833–1888 and 833–1521 of ZFP106 were also expressed as fusion proteins with green fluorescent protein (GFP) and their subcellular localization analyzed in living cells.

the N-terminal 411 or 781 residues of ZFP106a, or residues 2–810 of ZFP106b) were all efficiently transported into the nucleus, but not the nucleolus, despite the absence of a classical, positively charged NLS. These findings were in line with a neural network analysis (Reinhardt & Hubbard, 1998) of the amino acids 1–411 region, strongly predicting a nuclear localization of this ZFP106 fragment based on its overall amino acid composition. Furthermore, since ZFP106d was targeted to the nucleolus with the same efficiency as ZFP106a, the bipartite NLS (residues 803–819) was dispensable for nuclear import, at least of ZFP106d. Two motifs of ZFP106d fit experimentally determined NLS consensus sequences (Cokol, Nair, & Rost, 2000): one between residues 1052 and 1060 (KRRKikgKK) and another, with overlapping mono- and bipartite NLS, between residues 1361 and 1397. ZFP106 (837–1177) containing the first putative NLS exhibited nuclear import, but was absent from the nucleolus (Fig. 5D). In contrast, ZFP106 (1275–1655), containing the second potential NLS, was only detected in the cytoplasm. Likewise, ZFP106 (1177–1888), lacking the first putative NLS but retaining the second NLS and the C-terminal WD40 repeats was restricted to the cytoplasm, essentially ruling out a role of these C-terminal sequences for nuclear uptake. Hence, nuclear import of ZFP106d depends on the amino acids 837–1177 region containing a classical NLS motif at residues 1052–1060.

Since ZFP106 (837–1177) was excluded from the nucleoli, elements in the more C-terminal region, though not involved in nuclear import, seemed to be necessary for further targeting to the nucleolus. In several instances, nucleolar retention has been shown to require, in addition to a functional NLS, a second NLS-like cluster of basic residues (Annilo, Karis, Hoth, Rikk, Kruppa, & Metspalu, 1998; Russo, Ricciardelli, & Pietropaolo, 1997), suggesting that residues 1361–1397, while dispensable for nuclear uptake, might mediate nucleolar targeting. However, ZFP106 (833–1530) containing both aforementioned basic regions localized like ZFP106 (833–1177) to the nucleoplasm excluding the nucleolus. Similarly, fusion of either the WD40 repeats domain or the C-terminal zinc finger region to ZFP106 (833–1177) did not confer nucleolar targeting. Yet, a fusion protein of ZFP106 (833–1177) with amino acids 1528–1888 containing both the WD40 repeats domain and zinc finger motifs, accumulated exclusively in the nucleoli. Analysis of green fluorescent protein (GFP) fusion proteins in living cells were consistent with a nucleolar-targeting function of the amino acids 1528–1888 region (Fig. 5D). Collectively, the results of these experiments showed that nucleolar targeting of ZFP106d required the combination of two separate functional elements: an NLS within residues 833–1177 and the C-terminal WD40 repeats/zinc finger region, which functions as a nucleolar-targeting domain.

3.5. The nucleostemin-like protein TSG118 interacts with the nucleolar-targeting domain of ZFP106

The nucleolar localization of ZFP106 did not require ongoing rRNA synthesis, as it was retained in the segregated nucleoli after treatment with actinomycin D (Fig. 4A). Furthermore, ZFP106d was not extracted from the nucleolus by chromatin and RNA removal during in situ fractionation (Fig. 2F), suggesting that nucleic acid binding is not essential for nucleolar accumulation of ZFP106. Thus, the nucleolar-targeting function of the C-terminal WD40 repeats/zinc finger region likely involves interactions with other nucleolar proteins.

To identify such protein(s), we screened $\sim 1.3 \times 10^7$ clones of a mouse embryo cDNA library by the yeast two-hybrid method using as bait the C-terminal domain of ZFP106 (Fig. 6A). Sequence analysis of 56 positive clones revealed that 48 encoded six different C-terminal portions of testis-specific protein 118 (TSG118), a conserved mammalian protein expressed primarily in embryonic stem cells, spermatogenic cells, and somatic cell lines (Larsson et al., 1999). The TSG118 region interacting with the C-terminus of ZFP106 can be localized to amino acids 362–530, which are encoded by all TSG118 clones isolated (Fig. 6A). Of note, we also obtained TSG118 clones when the amino acids 837–1888 region of ZFP106 was employed as bait in a second library screen (data not shown). The specificity of the interaction in yeast was confirmed by two-hybrid assays using reversed crosses between yeast strains expressing different parts of ZFP106 fused to the Gal4 transcriptional activation domain and TSG118 fused to the Gal4 DNA-binding domain (Fig. 6B). Next, we used co-immunoprecipitation assays to determine whether this interaction also

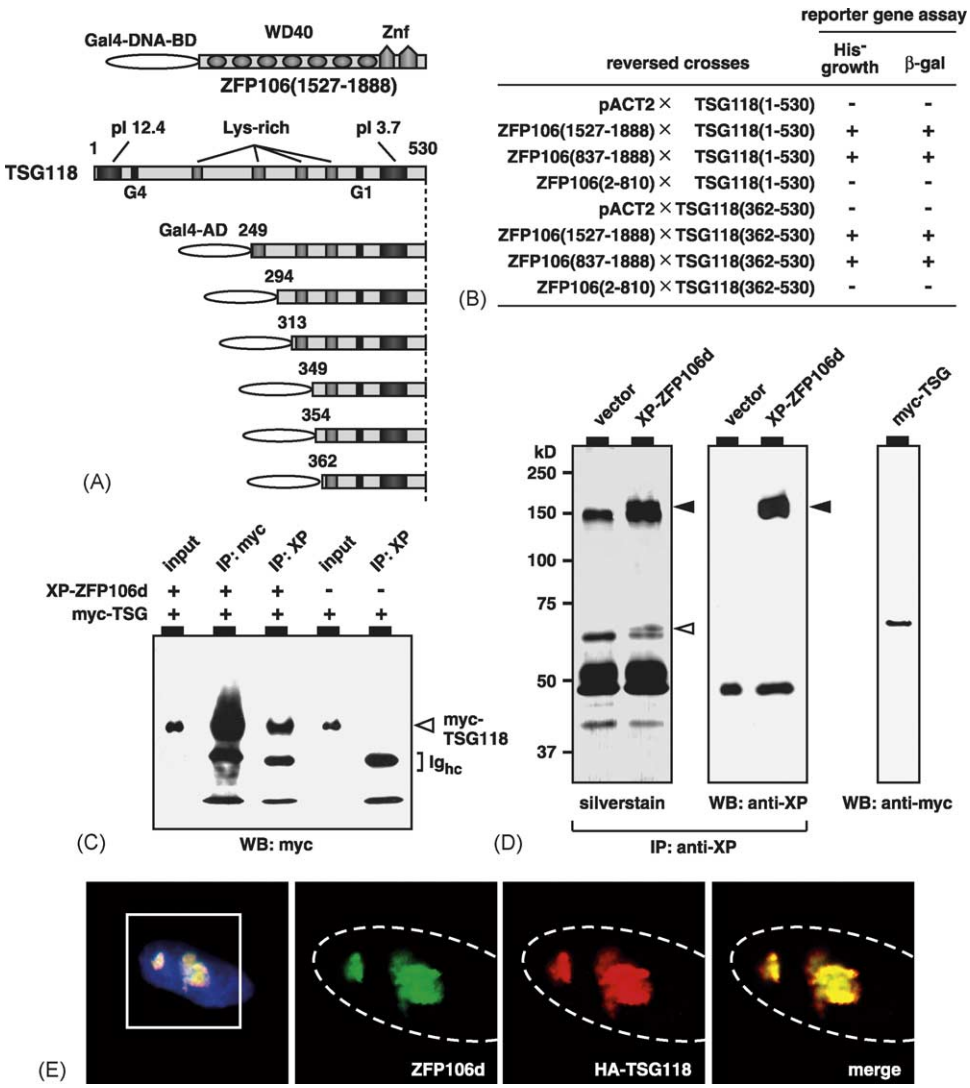

Fig. 6. Interaction of TSG118 with the nucleolar-targeting domain of ZFP106. (A) Schematic depicting the bait construct and the overlapping TSG118 cDNA clones obtained by screening a mouse embryonic library using the yeast two-hybrid method. BD, Gal4 DNA binding domain; AD, Gal4 transcriptional activation domain. (B) Crosses were made by mating AH109 (MATa) yeast harboring the first listed cDNA sequence fused to the AD sequence with Y187 (MATα) yeast expressing the second listed cDNA fused to the BD sequence. Numbers indicate the corresponding amino acid regions of ZFP106a or TSG118. Results of reporter gene assays refer to growth on minimal medium lacking histidine (His) and to expression of β-galactosidase activity (β-gal). (C) Solubilized nuclear fractions of HeLa cells expressing either myc-TSG118 alone or both myc-TSG118 and XP-ZFP106d were subjected to immunoprecipitation with anti-myc or anti-XP antibodies. Myc-TSG was only found in the anti-XP immunoprecipitate when XP-ZFP106d was co-expressed. Aliquots (1%) of the precleared lysates were loaded on the gel for comparison (input). (D) ZFP106d also co-precipitates an endogenous protein from HeLa nuclear extract. (E) HeLa cells were co-transfected with expression plasmids encoding HA-TSG118 and XP-ZFP106a (or XP-ZFP106d). The encoded proteins were visualized by indirect immunofluorescence and their co-localization examined by CLSM (regions of co-localization appear in yellow in the merged view).

occurred in mammalian cells. Under the lysis conditions employed, both myc-TSG and XP-ZFP106d could be partially recovered in the soluble nuclear fraction of HeLa cells transfected with the corresponding expression constructs. XP antibody co-precipitated myc-TSG118 only in the presence of co-transfected XP-ZFP106d (Fig. 6C) indicating that these proteins are found in the same complex in mammalian cells. As revealed by silver staining, ZFP106d also specifically co-precipitated an endogenous protein of HeLa cells matching the size of recombinant TSG118 (Fig. 6D).

A prerequisite for proteins to interact in vivo is their presence in the same intracellular compartment. TSG118 reportedly co-localizes with fibrillarin during the interphase of the somatic cell cycle and the meiotic phase of spermatogenesis (Larsson et al., 1999). By confocal imaging, HA-TSG118 and XP-ZFP106d exhibited an exact overlap of their nucleolar signals in both untreated (Fig. 6E) and actinomycin-D-treated cells (not shown).

3.6. Downregulation of TSG118 expression upon terminal differentiation coincides with loss of nucleolar ZFP106

If TSG118 is indeed involved in the nucleolar targeting of ZFP106, changes in TSG118 expression may affect the subcellular localization of ZFP106. Although Northern blot analysis of adult mouse tissues showed TSG118 expression restricted to testis (not shown), most of the TSG118 expressed sequence tags in GenBank have been isolated from stem cells, tumor tissues or transformed cell lines suggesting that TSG118 is expressed only in cells able to proliferate, but not in terminally differentiated cells. Consistent with this concept, the level of TSG118 mRNA dropped rapidly, within a single day, upon induction of terminal differentiation in C2C12 myoblasts (Fig. 7A). Importantly, this effect was not observed in other cell lines, where identical conditions are unable to trigger terminal differentiation (Larsson et al., 1999), and thus not caused by growth arrest or serum deprivation per se. To analyze the subcellular localization of ZFP106 during terminal differentiation, we transfected C2C12 myoblasts with recombinant adenovirus allowing inducible expression of ZFP106 constructs. We found that the localization of ZFP106a was nucleolar in myoblasts, but nucleoplasmic and progressively cytoplasmic when expression was induced in early (d1) or later (d2) stages of differentiation, respectively (Fig. 7B). The same phenomenon was also observed with the N-terminal truncated ZFP106d isoform, which retains the TSG118-interacting domain. In residual, unfused myoblasts, which failed to differentiate, ZFP106 was confined to the nucleolus, further suggesting that terminal differentiation is indeed linked to the observed loss of nucleolar ZFP106. It should be mentioned that a general decrease in nucleolar size accompanies terminal differentiation (Zahradka, Larson, & Sells, 1991), but that this was not evident by nucleolar labeling with anti-fibrillarin at the time points analyzed in our experiments (not shown). We conclude that, in this cellular model system, the nucleolar ZFP106–TSG118 interaction is a phenomenon of proliferating but not terminally differentiated cells.

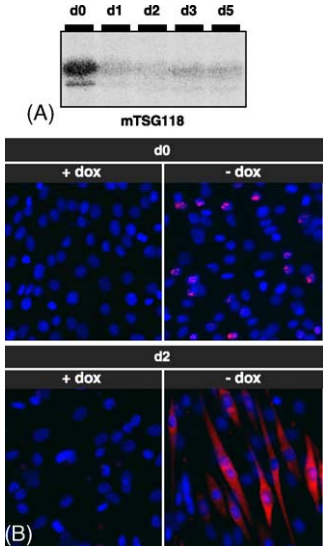

Fig. 7. Downregulation of TSG118 expression during differentiation coincides with loss of nucleolar ZFP106. (A) Northern blot showing rapid downregulation of TSG118 expression during the course of C2C12 myogenic differentiation. (B) C2C12 myoblasts were infected with recombinant adenovirus and kept for two days in either growth medium or differentiation medium, both with the addition of doxycycline (+dox) to suppress expression of XP-ZFP106d. Thereafter, both myoblasts (d0) and early myotubes (d2) were switched to doxycycline-free medium (−dox) for another 24 h to allow expression of XP-ZFP106d, before fixation and processing for immunofluorescence.

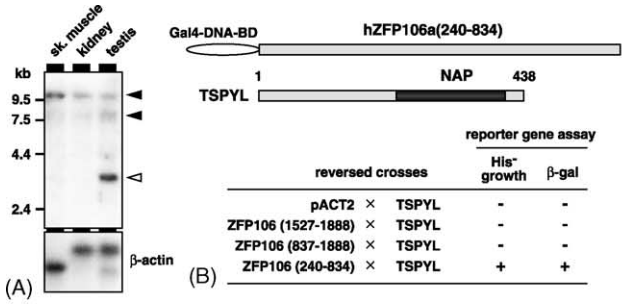
sk. muscle
kidney
testis
kb
9.5
7.5
4.4
2.4
β-actin
(A)
Gal4-DNA-BD
hZFP106a(240-834)
1
NAP
438
TSPYL
reporter gene assay
reversed crosses
His⁻ growth
β-gal
pACT2 × TSPYL - -
ZFP106 (1527-1888) × TSPYL - -
ZFP106 (837-1888) × TSPYL - -
ZFP106 (240-834) × TSPYL + +
(B)

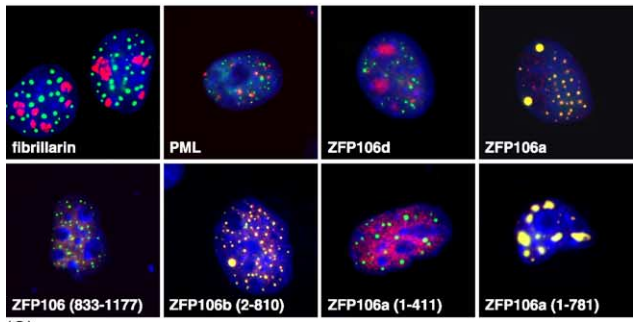
fibrillarin
PML
ZFP106d
ZFP106a
ZFP106 (833-1177)
ZFP106b (2-810)
ZFP106a (1-411)
ZFP106a (1-781)
(C)

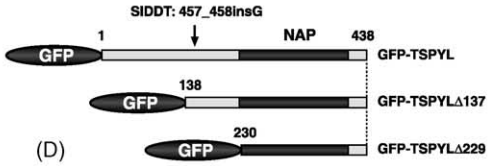
SIDDT: 457_458insG
1
NAP
438
GFP
GFP-TSPYL
138
GFP-TSPYLΔ137
230
GFP-TSPYLΔ229
(D)

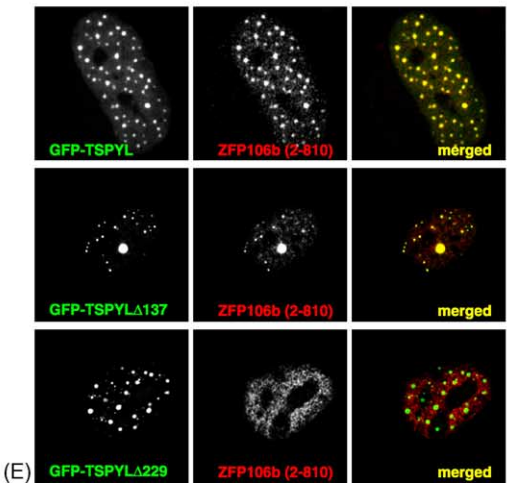
GFP-TSPYL
ZFP106b (2-810)
merged
GFP-TSPYLΔ137
ZFP106b (2-810)
merged
GFP-TSPYLΔ229
ZFP106b (2-810)
merged
(E)

3.7. Nucleoplasmic ZFP106 is recruited to TSPYL, a protein essential in testis development

Identification of TSG118 as ZFP106-interacting protein implicates ZFP106 in the differentiation of progenitor cells and/or testicular function. We had previously demonstrated expression of ZFP106 in testis using RT-PCR (Grasberger et al., 2005). By Northern blot analysis using probes covering different regions of the ZFP106 cDNA, we found that an alternative transcript is in fact expressed at highest levels in testis (Fig. 8A). This ∼3.7 kb mRNA was detected by both an exon 1/exon 2 probe (Fig. 8A) and an exon 3/exon 4 probe (not shown), but not with a probe against sequences downstream of exon 4. This finding prompted us to perform a two-hybrid screen using a corresponding region (amino acids 240–834) as bait (Fig. 8B). Out of $\sim 0.5 \times 10^6$ independent transformants, four clones were isolated, and sequence analysis revealed that one of them contained the full-length coding sequence of testis-specific Y-encoded-like protein (TSPYL). TSPYL is a widely expressed protein with a C-terminal nucleosome assembly protein (NAP) domain (Vogel, Dittrich, Mehraein, Dechend, Schnieders, & Schmidtke, 1998) and may function in chromatin remodeling and/or as transcriptional regulator during embryogenesis. Intriguingly, a homozygous truncation mutation in TSPYL, producing a truncated protein with loss of nuclear targeting, is responsible for a recently described syndrome of Sudden Infant Death with Dysgenesis of the Testis (SIDDT, OMIM 608800) (Puffenberger et al., 2004). The specificity of the interaction in yeast was confirmed by two-hybrid assays including vector-swapping analysis with TSPYL linked to the Gal4 DNA-binding domain (Fig. 8B). However, co-immunoprecipitation experiments in mammalian cells using epitope-tagged ZFP106 and TSPYL constructs gave ambiguous results, suggesting that a direct or indirect interaction between both proteins would be too weak to resist the lysis procedure required for solubilization. Furthermore, insolubility of both proteins expressed as GST fusions precluded demonstration of a direct protein–protein interaction in vitro. We reasoned that, even if the ZFP106–TSPYL interaction requires bridging by other molecule(s), such an association may nevertheless become manifest in a specific subcellular recruitment of both proteins. We therefore set out to study the localization of GFP-tagged TSPYL relative to ZFP106. As reported previously (Puffenberger et al., 2004), GFP-TSPYL localizes predominantly to the nucleoplasm forming symmetrical dots-like structures reminiscent of nuclear bodies. These TSPYL-positive bodies do not coincide with the morphologically similar PML nuclear bodies or Cajal bodies (Fig. 8C). In a small subset of cells (<5%), we observed nucleolar TSPYL, frequently associated with the absence of the smaller nucleoplasmic bodies (not shown). Double-immunofluorescence of GFP-TSPYL and various XP-tagged ZFP106 constructs revealed that ZFP106a co-localizes with TSPYL in the nucleoplasm, whereas TSPYL is not recruited into the nucleolus. In contrast, ZFP106d or fragments thereof with either nucleolar or nucleoplasmic distribution pattern (compare Fig. 5D) do not co-localize with TSPYL (Fig. 8C). This was expected, since these constructs lacked the N-terminal region of ZFP106 required for an interaction with TSPYL in yeast. Using deletion constructs of the latter region, we showed that the presence of ZFP106 residues 411–781 is critical for the co-localization with TSPYL (Fig. 8C). Likewise, deletion constructs of TSPYL (Fig. 8D) were assessed for co-localization with the amino acids 2–810 fragment of ZFP106, which is normally dispersed throughout the

Fig. 8. Recruitment of ZFP106 via an N-terminal domain into TSPYL-positive nuclear bodies. (A) Northern blot analysis of total RNA isolated from the indicated tissues using as probe the exon 1/exon 2 region of ZFP106. The open arrow marks a testis-specific ∼3.7 kb transcript. Hybridization with a β-actin control probe is shown at the bottom. (B) Schematic depicting the bait protein used to screen a human skeletal muscle library by the yeast two-hybrid method. Out of four clones isolated, one contained the complete coding sequence of TSPYL in frame to the Gal4 AD. Also shown are the results of confirmatory reporter gene assays using vector-swapping, i.e. with Gal4 BD-TSPYL and Gal4 AD-ZFP106 fusions. (C) Subnuclear localization of GFP-TSPYL relative to the ZFP106 constructs and markers of known nuclear bodies (nucleolus, Cajal bodies, and PML nuclear bodies). (D) Schematic of the GFP fusion constructs containing full-length or N-terminal truncated TSPYL. The arrow indicates the first amino acid (residue 153) affected by the frame-shift mutation (457_458insG) found in patients with testis dysgenesis. This mutation results in a truncated protein of 169 amino acids (Puffenberger et al., 2004). (E) CLSM analysis of the recruitment of ZFP106b (2–810) into nuclear bodies formed by the TSPYL constructs depicted in (D).

nucleoplasm (compare Fig. 5D). We found that the C-terminal region of TSPYL comprising the NAP domain is sufficient for both nuclear import and the formation of nuclear bodies, but that an adjacent N-terminal region (residues 138–229) is required for recruitment of ZFP106 (Fig. 8E). As shown in Fig. 8D, the integrity of the latter region of TSPYL is disrupted by the SIDDT mutation (457_458insG), which causes a frame-shift at codon 153 with cessation of translation at codon 169 (Puffenberger et al., 2004). Collectively, the experiments in yeast and the results of the recruitment studies support the view that ZFP106, at least indirectly, associates with TSPYL in mammalian cells and, thus, relates to a novel developmental pathway.

4. Discussion

In this report, we identified the WD40 repeats protein ZFP106 as an unusually large nucleolar matrix protein, which has not been recognized in previous proteomics studies of the nucleolus (Andersen et al., 2002; Scherl et al., 2002), and analyzed the mechanism of its subcellular targeting.

Although a recent, comprehensive sequence analysis of nucleolar proteins detected peculiarities in their amino acid composition (Leung, Andersen, Mann, & Lamond, 2003), e.g. the overrepresentation of GAR (glycine- and arginine-rich) regions, it did not reveal general nucleolar-targeting motifs. Rather, the current consensus view is that nucleolar targeting, in marked contrast to the active transport involved in nuclear import, is due to nucleolar retention by interactions with nucleic acid or protein constituents of the nucleolus (van Eenennaam et al., 2001). However, such interactions, which represent the molecular basis of nucleolar targeting, have been characterized for only a small subset of nucleolar proteins. For example, nucleolar localization of nucleolin depends on interaction with rRNA via its GAR domain (Heine, Rankin, & DiMario, 1993), and nuclear targeting of UBF is mediated by binding to rDNA (Maeda et al., 1992).

In the case of ZFP106, nuclear import depends on a region comprising a classical monopartite NLS, while nucleolar targeting requires, in addition, the ZFP106 C-terminus containing the WD40 domain, but not the presence of nucleolar RNA or DNA. The WD40 domain is among the most frequently encountered domains in the nucleolar proteome (Leung et al., 2003) and known to be a typical protein–protein interaction domain. Using the yeast two-hybrid method, we identified TSG118 (Larsson et al., 1999), a constitutive nucleolar protein of proliferating somatic cells, as binding partner for the ZFP106 C-terminal domain. TSG118 interacts and co-localizes with ZFP106 in the fibrillar regions of the nucleolus. Furthermore, correlation of TSG118 expression with the subcellular localization of ZFP106 during terminal differentiation (Fig. 7) provides circumstantial evidence that TSG118 is indeed involved in the nucleolar recruitment of ZFP106.

Although TSG118 does not display significant sequence homology to any protein of known function, a detailed statistical analysis of its amino acid composition (Brendel, Bucher, Nourbakhsh, Blaisdell, & Karlin, 1992) revealed that TSG118 is closely related to nucleostemin (Tsai & McKay, 2002). Both TSG118 and nucleostemin are constitutively nucleolar and have similar size (530 versus 538 amino acids of the murine proteins) and composition (e.g. isoelectric point [p*I*] 9.9 versus 9.4). All recognizable structural features of nucleostemin are shared by TSG118, which are the presence of multiple PSORT-predicted NLS, an N-terminal basic region (residues 2–46; p*I* 12.4 versus residues 13–43; p*I* 12.8), a C-terminal acidic domain (residues 460–503; p*I* 3.7 versus residues 349–443; p*I* 4.3), and a conserved G4 GTP-binding motif (KXDL). TSG118 also contains a motif (IXXXXGKT) related to the G1 motif (P-loop; [AG]XXXXGK[ST]) found in nucleostemin. When neuronal stem cells are triggered to differentiate, expression of nucleostemin decreases rapidly reflecting the kinetics of the decrease in TSG118 expression upon induction of myogenic differentiation. Akin to TSG118, nucleostemin is expressed in stem cells and several cancer cell lines, and, in adult tissues, at high level only in testis (Tsai & McKay, 2002). Nucleostemin appears to be important for self-renewal of progenitor cells, and the loss of its expression is related to the cell-cycle exit during terminal differentiation. Although, by immunofluorescence, nucleostemin is exclusively detected in the nucleoli, a small fraction appears to GTP-regulated shuttle between the nucleoli and the nucleoplasm, where it was found in complex with the tumor suppressor p53 and, thereby, presumably acts in a stem-cell-specific control of p53 (Tsai & McKay, 2002). It should be noted that ZFP106, via the P1 promoter, is like TSG118 and

nucleostemin expressed in stem cells, and has indeed been proposed as distinguishing marker for neuronal, mesenchymal, and germinal, but not haematological, stem cell populations (Sharov et al., 2003). The interaction with TSG118 in progenitor cells should therefore be relevant for P1-derived ZFP106 isoforms, but presumably not for those expressed from P2 since their expression is strictly coupled to the onset of muscle differentiation (Grasberger et al., 2005) and, thereby, complementary to the expression of TSG118 (Fig. 7A).

Additional two-hybrid screening with the N-terminal region of ZFP106, which is also encoded by an alternative transcript with high expression in testis, led to the isolation of TSPYL, an NAP domain protein. Although we do presently not have proof for a direct physical interaction between ZFP106 and TSPYL, subcellular recruitment studies showed that, consistent with our results in the yeast system, amino acids 411–781 of ZFP106 and amino acids 138–229 of TSPYL are crucial for the recruitment of nucleoplasmic ZFP106 into TSPYL-positive bodies. Considering that other NAP proteins are part of multi-protein complexes (Rodriguez, Ruiz, Price, & Zannis-Hadjopoulos, 2004), these data strongly imply that ZFP106 and TSPYL, if not in direct contact, are at least found in a common molecular complex in mammalian cells. A mutation in TSPYL is the cause of a sudden infant death syndrome with, in affected males, testis dysgenesis (SIDDT) suggesting that TSPYL is part of a novel pathway important in the development of the testis and likely other tissues, such as, the brain (Puffenberger et al., 2004). Other NAP domain proteins have been implicated in the control of mitotic events (Kellogg, Kikuchi, Fujii-Nakata, Turck, & Murray, 1995), nucleosome assembly (McQuibban, Commisso-Cappelli, & Lewis, 1998) or tissue-specific transcriptional regulation during development (Rogner, Spyropoulos, Le Novere, Changeux, & Avner, 2000). They may either repress transcription by facilitating nucleosome formation or promote transcription by removing histones from chromatin, thereby allowing sequence-specific transcriptional factors to bind to chromatin (Walter, Owen-Hughes, Cote, & Workman, 1995).

Based on our present findings, what could be the role of the interaction of ZFP106 with TSG118 in the nucleolus? While the close spatial association of ZFP106 with the rDNA transcription machinery is certainly compatible with a regulatory role of ZFP106 in rRNA synthesis or processing, ZFP106 did not, at least by overexpression of its isoforms, have obvious effects on the accumulation of rRNA transcripts. It is to be noted that a predominant localization in a specific, cellular compartment at steady state does not mean that the protein is acting exclusively there. The functionally more relevant interactions of ZFP106 may well take place in the nucleoplasm, e.g. with TSPYL, rather than in the nucleolus, and result in the formation of transient, unstable complexes. Thus, instead of participation in a specific nucleolar function, the presence of ZFP106 in the nucleolus may reflect the regulation of ZFP106 activity by its sequestration, prior to terminal differentiation, in the only nuclear compartment lacking the proteasome (Reits, Benham, Plougastel, Neefjes, & Trowsdale, 1997; Rivett, 1998). Upon release from the nucleolus at the onset of differentiation, ZFP106 in conjunction with TSPYL may then have a transient function, e.g. in the regulation of specific developmental genes or region-specific chromatin remodeling. Clearly, the identification of protein–protein interactions described here provides exciting new entry points for elucidating the role of ZFP106 in development and the pathogenesis of SIDDT.

References

Andersen, J. S., Lyon, C. E., Fox, A. H., Leung, A. K., Lam, Y. W., Steen, H., et al. (2002). Directed proteomic analysis of the human nucleolus. *Current Biology*, *12*, 1–11.

Annilo, T., Karis, A., Hoth, S., Rikk, T., Kruppa, J., & Metspalu, A. (1998). Nuclear import and nucleolar accumulation of the human ribosomal protein S7 depends on both a minimal nuclear localization sequence and an adjacent basic region. *Biochemical and Biophysical Research Communications*, *249*, 759–766.

Bernardi, R., Scaglioni, P. P., Bergmann, S., Horn, H. F., Vousden, K. H., & Pandolfi, P. P. (2004). PML regulates p53 stability by sequestering Mdm2 to the nucleolus. *Nature Cell Biology*, *6*, 665–672.

Brendel, V., Bucher, P., Nourbakhsh, I. R., Blaisdell, B. E., & Karlin, S. (1992). Methods and algorithms for statistical analysis of protein sequences. *Proceedings of the National Academy of Sciences of the United States of America*, *89*, 2002–2006.

Cokol, M., Nair, R., & Rost, B. (2000). Finding nuclear localization signals. *EMBO Reports*, *1*, 411–415.

Fatyol, K., & Szalay, A. A. (2001). The p14ARF tumor suppressor protein facilitates nucleolar sequestration of hypoxia-inducible factor-1alpha (HIF-1alpha) and inhibits HIF-1-mediated transcription. *Journal of Biological Chemistry*, *276*, 28421–28429.

Gebrane-Younes, J., Fomproix, N., & Hernandez-Verdun, D. (1997). When rDNA transcription is arrested during mitosis, UBF is still associated with non-condensed rDNA. *Journal of Cell Science*, *110*(Part 19), 2429–2440.

Grasberger, H., Ye, H., Mashima, H., & Bell, G. I. (2005). Dual promoter structure of ZFP106: regulation by myogenin and nuclear respiratory factor-1. *Gene*, *344*, 143–159.

Hall, R., Hyde, J. E., Goman, M., Simmons, D. L., Hope, I. A., Mackay, M., et al. (1984). Major surface antigen gene of a human malaria parasite cloned and expressed in bacteria. *Nature*, *311*, 379–382.

Harlow, E., & Lane, D. (1988). *Antibodies: A laboratory manual*. Cold Spring Harbor, NY: Cold Spring Harbor Laboratory Press.

He, D. C., Nickerson, J. A., & Penman, S. (1990). Core filaments of the nuclear matrix. *Journal of Cell Biology*, *110*, 569–580.

Heine, M. A., Rankin, M. L., & DiMario, P. J. (1993). The Gly/Arg-rich (GAR) domain of Xenopus nucleolin facilitates in vitro nucleic acid binding and in vivo nucleolar localization. *Molecular Biology of the Cell*, *4*, 1189–1204.

Jacobson, M. R., Cao, L. G., Wang, Y. L., & Pederson, T. (1995). Dynamic localization of RNase MRP RNA in the nucleolus observed by fluorescent RNA cytochemistry in living cells. *Journal of Cell Biology*, *131*, 1649–1658.

Kellogg, D. R., Kikuchi, A., Fujii-Nakata, T., Turck, C. W., & Murray, A. W. (1995). Members of the NAP/SET family of proteins interact specifically with B-type cyclins. *Journal of Cell Biology*, *130*, 661–673.

Larsson, M., Brundell, E., Jorgensen, P. M., Stahl, S., & Hoog, C. (1999). Characterization of a novel nucleolar protein that transiently associates with the condensed chromosomes in mitotic cells. *European Journal of Cell Biology*, *78*, 382–390.

Leung, A. K., Andersen, J. S., Mann, M., & Lamond, A. I. (2003). Bioinformatic analysis of the nucleolus. *Biochemical Journal*, *376*, 553–569.

Lin, D. Y., & Shih, H. M. (2002). Essential role of the 58-kDa microspherule protein in the modulation of Daxx-dependent transcriptional repression as revealed by nucleolar sequestration. *Journal of Biological Chemistry*, *277*, 25446–25456.

Maeda, Y., Hisatake, K., Kondo, T., Hanada, K., Song, C. Z., Nishimura, T., et al. (1992). Mouse rRNA gene transcription factor mUBF requires both HMG-box1 and an acidic tail for nucleolar accumulation: molecular analysis of the nucleolar targeting mechanism. *EMBO Journal*, *11*, 3695–3704.

McQuibban, G. A., Commisso-Cappelli, C. N., & Lewis, P. N. (1998). Assembly, remodeling, and histone binding capabilities of yeast nucleosome assembly protein 1. *Journal of Biological Chemistry*, *273*, 6582–6590.

Mekhail, K., Gunaratnam, L., Bonicalzi, M. E., & Lee, S. (2004). HIF activation by pH-dependent nucleolar sequestration of VHL. *Nature Cell Biology*, *6*, 642–647.

Misteli, T. (2001). Protein dynamics: implications for nuclear architecture and gene expression. *Science*, *291*, 843–847.

Puffenberger, E. G., Hu-Lince, D., Parod, J. M., Craig, D. W., Dobrin, S. E., Conway, A. R., et al. (2004). Mapping of sudden infant death with dysgenesis of the testes syndrome (SIDDT) by an SNP genome scan and identification of TSPYL loss of function. *Proceedings of the National Academy of Sciences of the United States of America*, *101*, 11689–11694.

Reinhardt, A., & Hubbard, T. (1998). Using neural networks for prediction of the subcellular location of proteins. *Nucleic Acids Research*, *26*, 2230–2236.

Reits, E. A., Benham, A. M., Plougastel, B., Neefjes, J., & Trowsdale, J. (1997). Dynamics of proteasome distribution in living cells. *EMBO Journal*, *16*, 6087–6094.

Rivett, A. J. (1998). Intracellular distribution of proteasomes. *Current Opinion in Immunology*, *10*, 110–114.

Rodriguez, P., Ruiz, M. T., Price, G. B., & Zannis-Hadjopoulos, M. (2004). NAP-2 is part of multi-protein complexes in HeLa cells. *Journal of Cellular Biochemistry*, *93*, 398–408.

Rogner, U. C., Spyropoulos, D. D., Le Novere, N., Changeux, J. P., & Avner, P. (2000). Control of neurulation by the nucleosome assembly protein-1-like 2. *Nature Genetics*, *25*, 431–435.

Russo, G., Ricciardelli, G., & Pietropaolo, C. (1997). Different domains cooperate to target the human ribosomal L7a protein to the nucleus and to the nucleoli. *Journal of Biological Chemistry*, *272*, 5229–5235.

Sambrook, J., Fritsch, E. F., & Maniatis, T. (1989). *Molecular cloning: A laboratory manual* (2nd ed.). Cold Spring Harbor, NY: Cold Spring Harbor Laboratory Press.

Scheer, U., & Hock, R. (1999). Structure and function of the nucleolus. *Current Opinion in Cell Biology*, *11*, 385–390.

Scherl, A., Coute, Y., Deon, C., Calle, A., Kindbeiter, K., Sanchez, J. C., et al. (2002). Functional proteomic analysis of human nucleolus. *Molecular Biology of the Cell*, *13*, 4100–4109.

Schreiber, E., Matthias, P., Muller, M. M., & Schaffner, W. (1989). Rapid detection of octamer binding proteins with 'mini-extracts', prepared from a small number of cells. *Nucleic Acids Research*, *17*, 6419.

Sharov, A. A., Piao, Y., Matoba, R., Dudekula, D. B., Qian, Y., VanBuren, V., et al. (2003). Transcriptome analysis of mouse stem cells and early embryos. *PLoS Biology*, *1*, 74.

Shaw, P. J., & Jordan, E. G. (1995). The nucleolus. *Annual Review of Cell and Developmental Biology*, *11*, 93–121.

Shou, W., Seol, J. H., Shevchenko, A., Baskerville, C., Moazed, D., Chen, Z. W., et al. (1999). Exit from mitosis is triggered by Tem1-dependent release of the protein phosphatase Cdc14 from nucleolar RENT complex. *Cell*, *97*, 233–244.

Tsai, R. Y., & McKay, R. D. (2002). A nucleolar mechanism controlling cell proliferation in stem cells and cancer cells. *Genes & Development*, *16*, 2991–3003.

van Eenennaam, H., van der Heijden, A., Janssen, R. J., van Venrooij, W. J., & Pruijn, G. J. (2001). Basic domains target protein subunits of the RNase MRP complex to the nucleolus independently of complex association. *Molecular Biology of the Cell*, *12*, 3680–3689.

Visintin, R., & Amon, A. (2000). The nucleolus: the magician's hat for cell cycle tricks. *Current Opinion in Cell Biology*, *12*, 372–377.

Vogel, T., Dittrich, O., Mehraein, Y., Dechend, F., Schnieders, F., & Schmidtke, J. (1998). Murine and human TSPYL genes: novel

members of the TSPY-SET-NAP1L1 family. *Cytogenetics and Cell Genetics*, *81*, 265–270.

Walter, P. P., Owen-Hughes, T. A., Cote, J., & Workman, J. L. (1995). Stimulation of transcription factor binding and histone displacement by nucleosome assembly protein 1 and nucleoplasmin requires disruption of the histone octamer. *Molecular and Cellular Biology*, *15*, 6178–6187.

Wansink, D. G., Schul, W., van der Kraan, I., van Steensel, B., van Driel, R., & de Jong, L. (1993). Fluorescent labeling of nascent RNA reveals transcription by RNA polymerase II in domains scattered throughout the nucleus. *Journal of Cell Biology*, *122*, 283–293.

Weber, J. D., Taylor, L. J., Roussel, M. F., Sherr, C. J., & Bar-Sagi, D. (1999). Nucleolar Arf sequesters Mdm2 and activates p53. *Nature Cell Biology*, *1*, 20–26.

Yokoyama, Y., Niwa, K., & Tamaya, T. (1992). Scattering of the silver-stained proteins of nucleolar organizer regions in Ishikawa cells by actinomycin D. *Experimental Cell Research*, *202*, 77–86.

Zahradka, P., Larson, D. E., & Sells, B. H. (1991). Regulation of ribosome biogenesis in differentiated rat myotubes. *Molecular and Cellular Biochemistry*, *104*, 189–194.

Zhang, Y., & Xiong, Y. (1999). Mutations in human ARF exon 2 disrupt its nucleolar localization and impair its ability to block nuclear export of MDM2 and p53. *Molecular Cell*, *3*, 579–591.

Zuberi, A. R., Christianson, G. J., Mendoza, L. M., Shastri, N., & Roopenian, D. C. (1998). Positional cloning and molecular characterization of an immunodominant cytotoxic determinant of the mouse H3 minor histocompatibility complex. *Immunity*, *9*, 687–698.